HHS Public Access

Author manuscript

Chem Res Toxicol. Author manuscript; available in PMC 2022 March 23.

Published in final edited form as:

Chem Res Toxicol. 2021 April 19; 34(4): 992–1003. doi:10.1021/acs.chemrestox.1c00013.

Identification of an *N*′-Nitrosonornicotine-specific Deoxyadenosine Adduct in Rat Liver and Lung DNA

Yupeng Li, **Stephen S. Hecht***

Masonic Cancer Center, University of Minnesota, Minneapolis, Minnesota 55455, United States.

Abstract

The tobacco specific nitrosamines *N*′-nitrosonornicotine (NNN) and 4-(methylnitrosamino)-1-(3-pyridyl)-1-butanone (NNK) are considered to be two of the most important carcinogens in unburned tobacco and its smoke. They readily cause tumors in laboratory animals and are classified as "carcinogenic to humans" by the International Agency for Research on Cancer. DNA adduct formation by these two carcinogens is believed to play a critical role in tobacco carcinogenesis. Among all the DNA adducts formed by NNN and NNK, 2′-deoxyadenosine (dAdo)-derived adducts have not been fully characterized. In the study reported here, we characterized the formation of N^6-[4-(3-pyridyl)-4-oxo-1-butyl]-2′-deoxyadenosine (N^6-POB-dAdo) and its reduced form N^6-PHB-dAdo formed by NNN 2′-hydroxylation in rat liver and lung DNA. More importantly, we characterized a new dAdo adduct N^6-[4-hydroxy-1-(pyridine-3-yl)butyl]-2′-deoxyadenosine (N^6-HPB-dAdo) formed after $NaBH_3CN$ or $NaBH_4$ reduction both *in vitro* in calf thymus DNA reacted with 5′-acetoxy-*N*′-nitrosonornicotine and *in vivo* in rat liver and lung upon treatment with NNN. This adduct was specifically formed by NNN 5′-hydroxylation. Chemical standards of N^6-HPB-dAdo and the corresponding isotopically labelled internal standard [pyridine-D_4]N^6-HPB-dAdo were synthesized using a four-step method. Both NMR and high resolution mass spectrometry data agreed well with the proposed structure of N^6-HPB-dAdo. The new adduct co-eluted with the synthesized internal standard under various LC conditions. Its product ion patterns of MS^2 and MS^3 transitions were also consistent with the proposed fragmentation patterns. Chromatographic resolution of the two diastereomers of N^6-HPB-dAdo was successfully achieved. Quantitation suggested a dose-dependent response of the levels of this new adduct in the liver and lung of rats treated with NNN. However, its level was lower than that of 2-[2-(3-pyridyl)-*N*-pyrrolidinyl]-2′-deoxyinosine (Py-Py-dI), a previously reported dGuo adduct that is also formed from NNN 5′-hydroxylation. The identification of

*To whom correspondence should be addressed: Masonic Cancer Center, University of Minnesota, 2231 6th Street SE - 2-148 CCRB, Minneapolis, MN 55455, USA. phone: (612) 624-7604; fax: (612) 624-3869; hecht002@umn.edu.

Supporting Information

The Supporting Information is available free of charge on the ACS Publications website at www.acs.org:

Synthetic details for 5′-acetoxyNNN and N^6-PHB-dAdo (Schemes S1–2); proposed mechanisms of formation of Py-Py-dN, N^6-HPB-dAdo and N^6-HPB-dAdo upon reduction of treated calf thymus DNA (Scheme S3); NMR spectra of 5′-acetoxyNNN, N^6-HPB-dAdo, [pyridine-D_4]N^6-HPB-dAdo, N^6-POB-dAdo, and N^6-PHB-dAdo (Figures S1–4); HPLC traces of N^6-POB-dAdo and N^6-PHB-dAdo (Figure S5); preliminary result of investigating new dAdo adducts in rat liver after reduction (Figure S6); fragmentation pattern comparison between N^6-PHB-dAdo and the new peak (Figure S7); compromised HPLC separation results as column quality decreased (Figure S8); formation of N^6-POB-dAdo in unreduced DNA samples (Figure S9); formation of N^6-PHB-dAdo and N^6-HPB-dAdo in DNA samples reduced by $NaBH_3CN$ (Figure S10); calibration curve for N^6-HPB-dAdo (Figure S11); HPLC flow rate and gradient composition at different time points in the LC-NSI-HRMS/MS method and the preliminary LC method (Tables S1–2).

The authors declare no competing financial interest.

N^6-HPB-dAdo in this study leads to new insights pertinent to the mechanism of carcinogenesis by NNN, and to the development of biomarkers of NNN metabolic activation.

Graphical Abstract

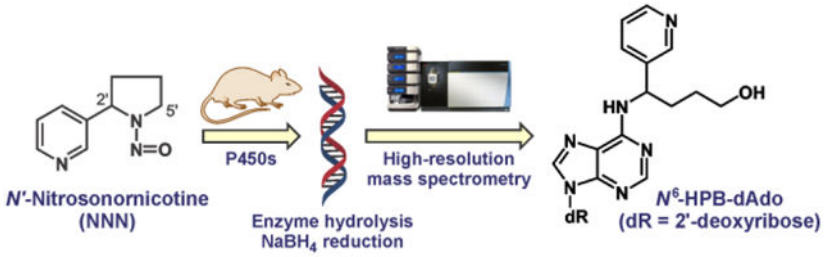

INTRODUCTION

Cigarette smoking remains the strongest single risk factor for cancer in the United States, accounting for 19% of all cancer cases and 29% of all cancer deaths.[1] Among the multiple carcinogens identified in both tobacco and tobacco smoke, the tobacco-specific nitrosamines *N*′-nitrosonornicotine (NNN, Scheme 1) and 4-(methylnitrosamino)-1-(3-pyridyl)-1-butanone (NNK) are among the most abundant.[2] In laboratory animals including rats, Syrian golden hamsters and mink, target tissues of NNN treatment are predominantly esophagus, oral mucosa, trachea, and nasal mucosa.[3] NNN is the most abundant oral carcinogen in smokeless tobacco, an established cause of oral cavity cancer in smokeless tobacco users.[4] Epidemiological studies have provided strong evidence that urinary levels of NNN in cigarette smokers predict future esophageal cancer incidence.[5,6] The International Agency for Research on Cancer has classified NNN and NNK as group 1 carcinogens ("carcinogenic to humans").[7]

DNA adduct formation plays a critical role in the process of tobacco carcinogenesis.[8] To exert their carcinogenicity, NNN and NNK require metabolic activation by cytochrome P450s (Scheme 1).[3,9] Initial hydroxylation of the carbons adjacent to the nitroso group of NNN forms 2′-hydroxyNNN (**5**) and 5′-hydroxyNNN (**6**). They spontaneously yield the reactive intermediate diazonium ions **9** and **10** as a consequence of two-step reactions including pyrrolidine ring opening and loss of H_2O. Similarly, the diazonium ion **9** can also be formed from α-methyl hydroxylation of NNK via the intermediate α-hydroxymethylNNK (**4**).

DNA is alkylated by these diazonium ions to form a panel of adducted products on both the nucleobases[10–19] and phosphate backbone.[20–23] Figure 1 summarizes recent progress towards identifying new pyridyl DNA adducts derived from NNN and NNK metabolism upon reaction with four nucleobases *in vitro* and *in vivo*. Among these, 2′-deoxyadenosine (dAdo)-derived adducts represent a small portion and are reported in quite low abundance in rat tissues. Three dAdo-derived adducts (**11**-**13**, Scheme 1) have been identified in tissues of rats treated with NNN, NNK, or the NNK metabolite 4-(methylnitrosamino)-1-(3-pyridyl)-1-butanol (NNAL).

N^6-[4-(3-Pyridyl)-4-oxo-1-butyl]-2′-deoxyadenosine (**11**, N^6-POB-dAdo) formed by NNK, and N^6-[4-(3-pyridyl)-4-hydroxy-1-butyl]-2′-deoxyadenosine (**12**, N^6-PHB-dAdo) formed by NNK and NNAL were characterized and quantified in rat liver and rat lung.[18] Their levels were significantly lower than 7-POB-Gua/7-PHB-Gua and O^2-POB-Thd/O^2-PHB-Thd (structures shown in Figure 1). For example, in the lung DNA of rats treated with 5 ppm NNK in the drinking water for 50 weeks, the level of N^6-POB-dAdo was 99 ± 3 fmol/mg DNA. However, the levels of 7-POB-Gua and O^2-POB-Thd in the same tissue were 688 ± 65 fmol/mg DNA and 4409 ± 320 fmol/mg DNA, respectively. Similarly, the level of N^6-PHB-dAdo was 35 ± 5 fmol/mg DNA, while the levels of 7-PHB-Gua and O^2-PHB-Thd were 129 ± 34 fmol/mg DNA and 1259 ± 66 fmol/mg DNA, respectively from the same rat lung tissue. The other adduct 6-[2-(3-pyridyl)-*N*-pyrrolidinyl]-2′-deoxynebularine (**13**, Py-Py-dN) formed through NNN 5′-hydroxylation followed by $NaBH_3CN$ reduction was identified in rat lung and rat nasal mucosa but in levels too low to quantify.[15] Collectively, these data seemed to indicate the unfavorable formation of dAdo-derived adducts by NNN and NNK. However, studies with other chemical carcinogens such as aristolochic acid[24] and colibactin[25] provided good evidence of the formation of dAdo-derived adducts. These data encouraged us to examine dAdo-derived adduct formation more thoroughly both *in vitro* and *in vivo*.

Considering the convergence of the same alkylating diazonium ion **9** formed by NNK α-methyl hydroxylation and NNN 2′-hydroxylation, the dAdo adducts N^6-POB-dAdo (**11**) and N^6-PHB-dAdo (**12**, after reduction) were expected to be similarly formed in the tissues of rats treated with NNN. However, our previous study using a method with relatively low sensitivity suggested only the presence of low levels of Py-Py-dN (**13**) in rat tissues after $NaBH_3CN$ reduction.[15] The apparent absence of N^6-PHB-dAdo (**12**) formed by NNN 2′-hydroxylation and the possible formation of the open-chain adduct N^6-[4-hydroxy-1-(pyridine-3-yl)butyl]-2′-deoxyadenosine (N^6-HPB-dAdo, **14**) formed by NNN 5′-hydroxylation (both after reduction) encouraged us to investigate these adducts using a new highly sensitive and specific liquid chromatography-nanoelectrospray ionization-high-resolution tandem mass spectrometry (LC-NSI-HRMS/MS) method. We found that N^6-PHB-dAdo (**12**) was formed after $NaBH_4$ reduction in the liver and lung of rats treated with racemic NNN in the drinking water for 3 weeks. Its precursor adduct N^6-POB-dAdo (**11**) was similarly observed in the rat tissues. However, both of these adducts occurred in very low abundance. Surprisingly, a new DNA adduct nearly co-eluting with N^6-PHB-dAdo was observed both *in vitro* and *in vivo* in relatively high abundance. It was characterized as the open-chain adduct N^6-HPB-dAdo (**14**) using the authentic synthesized standard, and its levels in the liver and lung of rats treated with NNN were quantified. This structurally new NNN-specific adduct N^6-HPB-dAdo leads to new insights for understanding mechanisms of carcinogenesis by tobacco-specific nitrosamines.

MATERIALS AND METHODS

Caution:

NNN and 5′-acetoxyNNN are strongly carcinogenic. They should be handled in a well-ventilated fume hood with extreme caution and with appropriate protective equipment.

Chemicals and supplies:

5′-Acetoxy-*N*′-nitrosonornicotine (5′-acetoxyNNN) was synthesized as reported previously.[15,26] $\mathcal{N}^6$-PHB-dAdo was synthesized as described before.[27] The isotopically labelled internal standards [pyridine-D_4]$\mathcal{N}^6$-POB-dAdo and [$^{15}N_5$]$\mathcal{N}^6$-PHB-dAdo were available from our previous study.[18] $\mathcal{N}^6$-HPB-dAdo and [pyridine-D_4]$\mathcal{N}^6$-HPB-dAdo were synthesized as described below. 3-Bromopyridine-D_4 (catalog number D-6066, lot number EF-132, purity of 99.1%-d_4) was purchased from CDN Isotopes Inc. (Quebec, Canada). 6-Chloropurine-2-deoxyriboside (CAS number 4594-45-0) was procured from Alfa Aesar (Tewksbury, MA). DNA hydrolysis enzymes including deoxyribonuclease I (catalog number P4527-40KU), phosphodiesterase I (catalog number P3243-1VL, lot number SLCD8995, ≥ 100 units/vial) and alkaline phosphatase (Roche, catalog number 10567752001) were purchased from Sigma-Aldrich and purified before use.[23] Porcine liver esterase was obtained from Sigma-Aldrich (catalog number E3019-20KU, lot number SLBM1761V) and purified in the same way as the DNA hydrolysis enzymes before use. All other chemicals and supplies were purchased from Sigma-Aldrich or Fisher Scientific. Milli-Q water (Millipore) was routinely used unless otherwise mentioned.

General synthetic procedures:

All commercial reagents were used without further purification except where noted. Reactions were monitored routinely by TLC-UV or reverse phase HPLC. Polygram pre-coated silica gel TLC plates (40 × 80 mm, 0.2 mm thick) with 254 nm fluorescence indicator were utilized. Products were purified through silica gel column chromatography or reverse phase HPLC. NMR spectra were recorded on a Bruker AC 500 MHz spectrometer. Chemical shifts are reported as parts per million (ppm) using residual solvent peaks as the internal references. The first-order peak patterns are indicated as s (singlet), d (doublet), t (triplet), q (quadruplet), p (pentuplet). Complex non-first-order signals are indicated as m (multiplet).

Synthesis of 5′-acetoxyNNN (3):

5′-AcetoxyNNN was synthesized using the method described before.[15,26] The reaction details and ^{1}H NMR data can be found in the Supporting Information (Scheme S1 and Figure S1). NMR data were consistent with the reported values.

Synthesis of $\mathcal{N}^6$-HPB-dAdo (14):

The synthetic route is illustrated in Scheme 2. The reaction conditions are detailed below.

4-Hydroxy-1-(pyridin-3-yl)butan-1-one (16, HPB).—This compound was synthesized using the method reported before with slight modifications.[20,28] To a solution of 3-bromopyridine (2.5 mmol, 241 μL) in dry Et_2O (15 mL) was slowly added a solution of n-butyllithium (~1.6 M in hexanes) (3.75 mmol, 2.34 mL) at −78 °C under a nitrogen atmosphere. The solution was stirred for an additional 15 min at −78 °C and then a solution of γ-butyrolactone (2.5 mmol, 192 μL) in dry Et_2O (5 mL) was added dropwise. The reaction mixture was allowed to warm to room temperature and stirred for 2 h. After completion, saturated $NaHCO_3$ solution was added to quench the reaction. The mixture was extracted 3 times with EtOAc. The organic layers were combined and dried over anhydrous

Na_2SO_4. The solvent was evaporated, and the resulting crude product **16** was purified by flash silica gel column chromatography (EtOAc) as a yellow oil (227 mg, 55%). ^{1}H NMR (500 MHz, $CDCl_3$) δ 9.20 (d, *J* = 2.3 Hz, 1H, pyr-H_2), 8.78 (dd, *J* = 4.9, 1.7 Hz, 1H, pyr-H_6), 8.25 (dt, *J* = 8.0, 2.0 Hz, 1H, pyr-H_4), 7.43 (dd, *J* = 8.0, 4.8 Hz, 1H, pyr-H_5), 3.77 (t, *J* = 6.1 Hz, 2H, -C$\underline{H}_2$OH), 3.16 (t, *J* = 6.9 Hz, 2H, COC$\underline{H}_2$-), 2.05 (p, *J* = 6.5 Hz, 2H, -CH_2C$\underline{H}_2$$CH_2$-), 1.62 (s, 1H, OH).

(Z/E)-4-Hydroxy-1-(pyridin-3-yl)butan-1-one O-methyl oxime (17).—A solution of compound **16** (1.35 mmol, 223 mg), methoxyamine hydrochloride (1.62 mmol, 135 mg) and Na_2CO_3 (1.62 mmol, 172 mg) in EtOH (2 mL) was stirred at 80 °C for 1 h. The reaction mixture was cooled to room temperature before filtration. The filtrate was concentrated and purified by flash silica gel column chromatography (hexanes/EtOAc) to afford the desired product **17** as a light yellow oil, mixture of (*Z*)- and (*E*)-isomers (171 mg, 65%). ^{1}H NMR (500 MHz, $CDCl_3$) δ 8.89 (dd, *J* = 2.3, 0.9 Hz, 1H, pyr-H_2), 8.60 (dd, *J* = 4.8, 1.6 Hz, 1H, pyr-H_6), 7.98 (dt, *J* = 8.1, 2.0 Hz, 1H, pyr-H_4), 7.30 (ddd, *J* = 8.1, 4.8, 0.9 Hz, 1H, pyr-H_5), 4.02 (s, 3H, -OCH_3), 3.62 (t, *J* = 6.3 Hz, 2H, -CH_2OH), 2.89 (t, *J* = 7.3 Hz, 2H, -C=N(OMe)-C$\underline{H}_2$), 1.96 (s, 1H, -OH), 1.80 (ddd, *J* = 13.2, 7.3, 6.0 Hz, 2H, -C$\underline{H}_2$$CH_2$OH).

4-Amino-4-(pyridin-3-yl)butan-1-ol (18).—A solution of the oxime **17** (0.6 mmol, 116 mg) in THF (1.2 mL) was cooled in an ice bath. Borane-THF complex (1 M in THF) (1.8 mmol, 1.8 mL) was added dropwise. The resulting solution was allowed to warm to room temperature, stirred for 1 h, then heated at reflux for 2.5 h. After cooling in an ice bath, the mixture was treated with H_2O (1 mL) and 1 N NaOH (2 mL) sequentially. The mixture was again warmed to 65 °C for 1 h. After reaction, all the solvents were evaporated. The resulting residue was purified by flash silica gel column chromatography (DCM/MeOH) to afford the desired product **18** as a colorless oil (60 mg, 60%). ^{1}H NMR (500 MHz, $CDCl_3$) δ 8.58 (s, 1H, pyr-H_2), 8.51 (d, *J* = 5.7 Hz, 1H, pyr-H_6), 7.95 (d, *J* = 7.9 Hz, 1H, pyr-H_4), 7.48 (dd, *J* = 8.0, 5.7 Hz, 1H, pyr-H_5), 4.10 (dd, *J* = 7.6, 5.6 Hz, 1H, -C$\underline{H}$(NH_2)-), 3.67 (dt, *J* = 6.6, 5.0 Hz, 2H, -CH_2OH), 1.89 – 1.73 (m, 2H, -CH(NH_2)C$\underline{H}_2$-), 1.62 (ddt, *J* = 26.2, 13.6, 7.1 Hz, 2H, -C$\underline{H}_2$$CH_2$OH).

***N*^{6}-[4-Hydroxy-1-(pyridine-3-yl)butyl]-2′-deoxyadenosine (14, *N*^{6}-HPB-dAdo).—**A solution of 6-chloropurine-2′-deoxyribose (**19**) (0.35 mmol, 95 mg), compound **18** (0.35 mmol, 58 mg) and triethylamine (0.52 mmol, 73 μL) in DMF (1.0 mL) was stirred at 45 °C for 12 days. The reaction mixture was diluted with H_2O (0.5 mL) before subjecting it to reverse phase HPLC purification. HPLC was carried out with Waters Associates (Milford, MA) systems equipped with a Shimadzu SPD-10A 0.2 mm Prep UV-VIS detector set to 254 nm. Separation was performed using a Luna 5μm C18(2) 100A 250 × 10 mm column purchased from Phenomenex (Torrance, CA). A 50-min program was used, with a flow rate of 4 mL/min and a gradient starting from 10% MeOH in H_2O for 10 min, then ramping up to 90% MeOH in H_2O over 25 min. After holding at 90% MeOH in H_2O for 3 min, the gradient was returned to 10% MeOH in H_2O over 5 min. The instrument was equilibrated for 7 min before the next injection. The crude product was collected at the retention time of ~25 min as a colorless oil after evaporation of solvents. This crude product (containing 2 peaks) was further purified under isocratic conditions (45% MeOH in H_2O). The first

peak eluting at 5.8 min was collected; it contained the desired product **14** (16 mg, 11%). One-dimensional and two-dimensional NMR spectra of compound **14** are presented in supplemental Figure S2. ^{1}H NMR (500 MHz, DMSO-d_6) δ 8.65 (s, 1H, pyr-H_2), 8.40 (d, J = 4.9 Hz, 1H, pyr-H_6), 8.37 (d, J = 1.3 Hz, 1H, ade-H_8), 8.16 (s, 1H, ade-H_2), 7.86 (dd, J = 7.7, 2.2 Hz, 1H, pyr-H_4), 7.32 (dd, J = 7.9, 4.8 Hz, 1H, pyr-H_5), 6.33 (t, J = 6.9 Hz, 1H, 1′-H), 5.39 (s, 1H, pyr-C<u>H</u>(NH)-), 5.28 (d, J = 4.0 Hz, 1H, 3′-OH), 5.21 – 5.10 (m, 1H, 5′-OH), 4.42 (t, J = 5.2 Hz, 1H, -CH_2CH_2O<u>H</u>), 4.40 (s, 1H, 3′-H), 3.86 (d, J = 5.1 Hz, 1H, 4′-H), 3.60 (dd, J = 11.6, 4.8 Hz, 1H, 5′-H_a), 3.56 – 3.47 (m, 1H, 5′-H_b), 3.41 (p, J = 5.7 Hz, 2H, -CH(NH)C<u>H_2</u>-), 2.77 – 2.66 (m, 1H, 2′-H_a), 2.24 (ddd, J = 13.3, 6.1, 2.9 Hz, 1H, 2′-H_b), 2.01 (s, 1H, -CH_2C<u>H_{2a}</u>OH), 1.87 (s, 1H, -CH_2C<u>H_{2b}</u>OH), 1.55 (s, 1H, -C<u>H_{2a}</u>CH_2OH), 1.47 – 1.36 (m, 1H, -C<u>H_{2b}</u>CH_2OH). ^{13}C NMR (126 MHz, DMSO-d_6) δ 154.0 (ade-C_6), 152.2 (ade-C_2), 148.5 (overlapped, pyr-C_2 & ade-C_4), 147.9 (pyr-C_6), 139.6 (overlapped, pyr-C_3 & ade-C_8), 134.2 (pyr-C_4), 123.4 (pyr-C_5), 119.6 (ade-C_5), 88.0 ($C_{4'}$), 83.9 ($C_{1'}$), 70.9 ($C_{3'}$), 61.9 ($C_{5'}$), 60.3 (-CH(NH)<u>C</u>H_2-), 51.2 (-<u>C</u>H(NH)CH_2-), 39.8 ($C_{2'}$), 32.2 (-CH_2OH), 29.7 (-<u>C</u>H_2CH_2OH). HRMS (Orbitrap Fusion): $[M+H]^+$ calc'd 401.1932; found 401.1930.

Synthesis of [pyridine-D_4]N^6-HPB-dAdo (24):

This compound was synthesized similarly as N^6-HPB-dAdo, except starting with 3-bromopyridine-D_4 (Scheme 2).

[Pyridine-D_4]4-hydroxy-1-(pyridin-3-yl)butan-1-one (21, [pyridine-D_4]HPB).— Under an atmosphere of N_2, to a stirred solution of 3-bromopyridine-D_4 (**20**) (1.54 mmol, 0.25 g) in anhydrous Et_2O (3.0 mL) was added a solution of n-butyllithium (1.6 M in hexanes, 3.09 mmol, 1.93 mL) dropwise over 15 min at −78 °C. Then a solution of γ-butyrolactone (1.85 mmol, 142 μL) in Et_2O (2.0 mL) was added dropwise. The reaction was allowed to warm to room temperature and stirred for 2 h. After completion, the reaction mixture was quenched with saturated $NaHCO_3$ solution. The mixture was extracted with EtOAc 3 times. The combined organic layers were evaporated to dryness. The residue was purified by flash silica gel column chromatography (EtOAc) to afford the desired product **21** as a yellow oil (170 mg, 65%). ^{1}H NMR (500 MHz, DMSO-d_6) δ 4.51 (t, J = 5.2 Hz, 1H, -OH), 3.46 (q, J = 6.3 Hz, 2H, -C<u>H_2</u>OH), 3.09 (t, J = 7.2 Hz, 2H, -$COCH_2$-), 1.78 (p, J = 6.7 Hz, 2H, -C<u>H_2</u>CH_2OH). ^{13}C NMR (126 MHz, DMSO-d_6) δ 199.5 (C=O), 59.9 (-CH_2OH), 34.9 (CO<u>C</u>H_2-), 26.9 (-<u>C</u>H_2CH_2OH).

[Pyridine-D_4](Z/E)-4-hydroxy-1-(pyridin-3-yl)butan-1-one O-methyl oxime (22).— A solution of [pyridine-D_4]HPB (**21**) (0.2 mmol, 34 mg), methoxyamine hydrochloride (0.24 mmol, 20 mg) and sodium carbonate (0.24 mmol, 25.4 mg) in EtOH (1.0 mL) was stirred at 80 °C for 1 h. The mixture was concentrated and purified by flash silica gel column chromatography (hexanes/EtOAc). Pure fractions were concentrated to afford the desired product **22** as a colorless oil (16 mg, 40%). ^{1}H NMR (500 MHz, $CDCl_3$) δ 4.02 (s, 3H, -OCH_3), 3.62 (s, 2H, -CH_2OH), 2.89 (t, J = 7.3 Hz, 2H, -C=N(OMe)-C<u>H_2</u>), 2.04 (s, 1H, -OH), 1.86 – 1.75 (m, 2H, -C<u>H_2</u>CH_2OH). The other geometric isomer was also observed in the spectrum, accounting for 28% of the product mixture.

[Pyridine-D_4]4-amino-4-(pyridin-3-yl)butan-1-ol (23).—The oxime **22** (0.08 mmol, 16 mg) in THF (1.5 mL) was cooled in an ice water bath. Borane-THF complex (1 M in THF, 0.5 mmol, 0.5 mL) was added dropwise. Under the same workup condition as described above, the desired product **23** was obtained as a colorless oil (11 mg, 81%).

[Pyridine-D_4]N^6-[4-hydroxy-1-(pyridine-3-yl)butyl]-2′-deoxyadenosine (24, [pyridine-D_4]N^6-HPB-dAdo).—A solution of compound **19** (0.02 mmol, 5.4 mg), compound **23** (0.02 mmol, 3.4 mg) and triethylamine (0.03 mmol, 4.2 μL) in DMF (0.5 mL) was stirred at 60 °C for 3 days. Using the same HPLC conditions as described above, the desired product **24** was collected at the retention time of 25.3 min as a colorless oil after evaporation (1.3 mg, 16%). NMR of compound **24** see supplementary Figure S3. ^{1}H NMR (500 MHz, DMSO-d_6) δ 8.41 (s, 1H, -NHCH(pyridine)-), 8.37 (d, J = 1.3 Hz, 1H, ade-H_8), 8.16 (s, 1H, ade-H_2), 6.39 – 6.22 (m, 1H, 1′-H), 5.38 (s, 1H, -NHCH(pyridine)-), 5.29 (d, J = 3.8 Hz, 1H, 3′-OH), 5.21 – 5.11 (m, 1H, 5′-OH), 4.45 – 4.41 (t, J = 5.1 Hz, 0.5H, 3′-H_a), 4.40 (s, 1H, -CH_2CH_2OH), 4.35 (t, J = 5.1 Hz, 0.5H, 3′-H_b), 3.87 (s, 1H, 4′-H), 3.65 – 3.55 (m, 1H, 5′-H_a), 3.55 – 3.47 (m, 1H, 5′-H_b), 3.45 – 3.36 (m, 2H, -$CH_2CH_2CH_2$OH), 2.79 – 2.66 (m, 1H, 2′-H_a), 2.29 – 2.20 (m, 1H, 2′-H_b), 2.01 (s, 1H, -CH_{2a}OH), 1.87 (s, 1H, -CH_{2b}OH), 1.55 (s, 1H, -$CH_{2a}CH_2$OH), 1.42 (s, 1H, -$CH_{2b}CH_2$OH). HRMS (Orbitrap Fusion): $[M+H]^+$ calc'd 405.2183; found 405.2182. MS data suggested compound **24** contains ~ 0.5% unlabeled N^6-HPB-dAdo.

Alternate Synthesis of N^6-PHB-dAdo (12):

Two diastereomers can be formed during the synthesis of **12** using the method reported by us before.[18,27] However, the standard compound synthesized previously showed only one single peak upon HPLC purification and LC-MS analysis. To exclude the possibility that we missed one of the two isomers when performing the HPLC fraction collection, N^6-PHB-dAdo was re-synthesized using the method illustrated in Scheme S2.[27] The reaction details are described in Scheme S2; NMR spectra of N^6-PHB-dAdo and its precursor compound N^6-POB-dAdo are presented in Figure S4; HPLC traces of both N^6-POB-dAdo and N^6-PHB-dAdo are shown in Figure S5. The newly synthesized N^6-PHB-dAdo was essentially identical to the one synthesized before, with no chromatographic separation of the two diastereomers under any tested conditions.

Sample preparation for identifying dAdo-derived adducts *in vitro*:

Calf thymus DNA (2 mg) was dissolved in 1.0 mL of 0.1 M phosphate buffer (pH = 7.4). To the solution were added 5′-acetoxyNNN (2 mg, 8.5 μmol) and purified porcine liver esterase (4 units). The mixture was incubated at 37 °C overnight (20 h). The resulting mixture (1.0 mL) was washed 3 times with $CHCl_3$/isoamyl alcohol (24:1). Each time, 2 mL of the mixed solvent was added, and the mixture was vortexed thoroughly for 10 min before centrifuging at 4000 *g* for 15 min. The upper layer was then transferred to a 5 mL centrifuge tube prefilled with 0.2 mL 5 M NaCl solution. To the centrifuge tube was then added 1.5 mL of ice-cold isopropanol with gentle swirling to precipitate the DNA. The DNA was transferred to a 4 mL silanized glass vial and washed 2 times with 0.5 mL ice-cold 75% EtOH and 100% EtOH sequentially. The DNA was dried under a stream of N_2 yielding a white solid (crude weight: 1.9 mg) and stored at −20 °C until hydrolysis.

The isolated DNA was dissolved in 500 μL of 10 mM sodium succinate buffer containing 5 mM $CaCl_2$ (pH = 7.3). For the samples reduced with $NaBH_3CN$, 100 μL 20 mg/mL $NaBH_3CN$ in the succinate buffer were added to the DNA solution. The mixture was incubated at 37 °C for 1 h before adding the isotopically labelled standard [pyridine-D_4]N^6-HPB-dAdo (and [$^{15}N_5$]N^6-PHB-dAdo and [pyridine-D_4]N^6-POB-dAdo when necessary). For the unreduced samples, no reducing agent was added. Three purified DNA hydrolysis enzymes were added as follows: deoxyribonuclease I (0.4 units), phosphodiesterase I (0.1 units), and alkaline phosphatase (0.8 units). After incubating at 37 °C overnight, the hydrolysate was filtered through a Microcon-10kDa centrifugal filter unit (Millipore Sigma, MRCPRT010) at 14000 *g* for 60 min at 4 °C. For the samples reduced with $NaBH_4$, 100 μL 20 mg/mL $NaBH_4$ in the succinate buffer were added to the DNA hydrolysate and incubated at 37 °C for 1 h. The resulting solution was adjusted to pH ~8.0 with 50 μL 1 N HCl before centrifugal filtration.

Ten μL of the filtrate was taken for dGuo quantitation by HPLC as described before.[23] The HPLC method was modified to achieve a better separation of the four nucleotide peaks. Quantitation of dGuo was carried out with a Dionex UltiMate 3000 RSLCnano System (Thermo Scientific, Waltham, MA) with a UV detector set at 254 nm. A Luna® 5 μm C18(2) 100 Å capillary column (250 × 0.5 mm) (Phenomenex, Torrance, CA) was used with H_2O and MeOH as mobile phases. Starting from 5% MeOH in H_2O, a linear gradient was increased to 25% MeOH in H_2O over 10 min. The gradient ramped to 95% MeOH in H_2O within 3 min, and held at 95% MeOH in H_2O for 5 min, then returned to 5% MeOH in H_2O over 2 min. The system was equilibrated at 5% MeOH in H_2O for 8 min before the next injection. The injection volume was 2 μL and the flow rate was 15 μL/min. The amount of dGuo was determined by a standard calibration curve, and the amount of DNA was calculated by considering that dGuo comprises 22% of all nucleotides in rat DNA.[23]

The remaining filtrate was purified using a 30 mg Strata-X polymeric reversed phase SPE cartridge (1 mL, Phenomenex, catalog number 8B-S100-TAK, Torrance, CA). The cartridge was activated with MeOH (2 mL) and preconditioned with H_2O (2 mL) before loading the filtrate. The cartridge was washed with H_2O (2 mL) and 30% MeOH solution (2 mL) sequentially. Then 2 mL of 75% MeOH were applied to elute the analytes. The 75% MeOH fractions were concentrated by SpeedVac and reconstituted in 100 μL 10% CH_3CN solution (Fisher, Optima® H_2O and Optima® CH_3CN). The sample was transferred to a glass vial with a 300 μL insert and concentrated by SpeedVac to dryness. Ten μL of H_2O (Optima® H_2O) were added to reconstitute the analytes prior to mass spectrometric analysis.

Calf thymus DNA incubated with a precursor of hydroxymethylNNK, 4-[(acetoxymethyl) nitrosamino]-1-(3-pyridyl)-1-butanone (NNKOAc), was also used for the analysis of dAdo-derived adducts. The isolated DNA was obtained from our previous study.[20] The procedures of DNA enzymatic hydrolysis, dGuo quantitation, analyte enrichment and sample preparation prior to mass spectrometric analysis were essentially the same as described above.

Sample preparation for identifying dAdo-derived adducts *in vivo*:

The animal studies were approved by the University of Minnesota Institutional Animal Care and Use Committee and reported in detail previously.[15] In brief, liver and lung DNA from rats treated with 50 ppm, 100 ppm or 500 ppm of racemic NNN in the drinking water for 3 weeks were used for the analysis of dAdo-derived adducts. The control group rats were treated under the same conditions except for drinking only plain tap water. Total NNN exposures to the rats from the 50 ppm, 100ppm or 500 ppm groups over the 3 weeks were estimated as 21 mg, 41 mg and 128 mg per rat, respectively. All these DNA samples were obtained from our previous study. DNA hydrolysis, dGuo quantitation, analyte enrichment through solid phase extraction (SPE), and sample preparation prior to mass spectrometric analysis were performed using the protocol detailed above.

Liver and lung DNA of rats treated with 5 ppm NNK in the drinking water for 50 weeks were also used for the analysis of dAdo-derived adducts in this study. The isolated NNK-treated rat DNA samples were obtained from a previous study.[20] The protocol to prepare the samples for MS analysis was the same as described above.

Qualitative Analysis of dAdo-derived adducts by LC-NSI-HRMS/MS:

The hydrolysates of DNA from *in vitro* samples (5′-acetoxyNNN- or NNKOAc-incubated calf thymus DNA) or rat livers and lungs (NNN treatment, NNK treatment, or control group) were analyzed by a new LC-NSI-HRMS/MS method. An aliquot of 2 μL DNA hydrolysate was injected into a Dionex UltiMate 3000 RSLCnano UPLC system equipped with a 5 μL autosampler injection loop. The UPLC system was coupled to the nanospray ion source. Chromatographic separation was achieved using a capillary column (75 μm i.d., 15–22 cm length, 10 μm orifice) created by hand-packing a fused-silica emitter (New Objective, Woburn, MA) with 5 μm particle size XBridge BEH Luna C18 stationary phase (Waters, Milford, MA). The LC conditions are described in Table S1.

The samples were analyzed using a Thermo Scientific™ Orbitrap Fusion™ Tribrid™ Mass Spectrometer (Thermo Scientific, San Jose, CA) in the positive ion profile mode. Four experiments were included for each scan cycle for the qualitative analysis. They are full scan, targeted selected-ion monitoring (SIM) scan, targeted MS^2 scan, and targeted MS^3 scan. Exact masses of all the analytes and their characteristic transitions were summarized in Table 1. For the full scan experiment, the resolution of the Orbitrap detector was 7500; the scan range was *m/z* 100–1000; the maximum injection time was 20 ms. For the targeted SIM scan experiment, precursor ions of the analytes including *m/z* 401.2 for N^6-HPB-dAdo or N^6-PHB-dAdo, *m/z* 405.2 for [pyridine-D_4]N^6-HPB-dAdo; *m/z* 406.2 for [$^{15}N_5$]N^6-PHB-dAdo (only included for the qualitative analysis of the reduced samples); *m/z* 399.2 for N^6-POB-dAdo and (N^6-[5-(3-pyridyl)tetrahydrofuran-2-yl]-2′-deoxyadenosine (N^6-Py-THF-dAdo)[27]), *m/z* 403.2 for [pyridine-D_4]N^6-POB-dAdo (only included for the qualitative analysis of the unreduced samples) were isolated with a quadrupole isolation window of *m/z* 1.5. The resolution of the Orbitrap detector was 15000. The maximum injection time was 22 ms. For the targeted MS^2 scan experiment, the quadrupole isolation window for isolating the precursor ions listed above was 1.5 and 30% of the HCD collision energy was used in the ion routing multipole. The Orbitrap detector was set up with a resolution of 60000 and a

scan range of product ions of *m/z* 100–500. The maximum injection time was 118 ms. For the targeted MS^3 scan experiment, the first-generation precursor ions as listed above and in Table 1 were isolated with a quadrupole isolation window of *m/z* 2.0 and the HCD collision energy setting was 30%. The second-generation precursor ions were *m/z* 285.1 for N^6-HPB-Ade, *m/z* 289.2 for [pyridine-D_4]N^6-HPB-Ade; *m/z* 267.1 for N^6-PHB-Ade, and *m/z* 272.1 for [$^{15}N_5$]N^6-PHB-Ade (only included for the qualitative analysis of the reduced samples); *m/z* 265.1 for N^6-POB-Ade with a H_2O loss, and *m/z* 269.1 for [pyridine-D_4]N^6-POB-Ade with a H_2O loss (only included for the qualitative analysis of the unreduced samples). They were isolated with a quadruple isolation window of *m/z* 1.5 and the HCD collision energy setting was 50%. The resolution of the Orbitrap detector was 30000. The scan range of the product ions was *m/z* 100–500. The maximum injection time was 54 ms. For all 4 experiments, the normalized AGC target (%) setting was chosen as "standard" (5×10^4) and the RF lens (%) setting was 60. The number of micro-scans was set as 1. The spray voltage was 2.2 KV. The ion transfer tube temperature was 300 °C. The EASY-IC™ internal mass calibration feature was used to ensure maximum mass accuracy. Extraction of precursor ion signals and product ion signals was performed with an accurate mass tolerance of 5 ppm. Thermo Xcalibur Qual Browser (version 4.3.73.11) was used to process all the MS data.

Quantitative analysis of N^6-HPB-dAdo in rat liver and rat lung:

The hydrolysates of DNA from the rat livers and lungs were analyzed by the LC-NSI-HRMS/MS method similarly as described above. Modifications of MS parameters were made to further increase the method sensitivity and specificity. Only two experiments were included for each scan cycle of the quantitation method. They are full scan and targeted MS^2 scan. For the full scan, the maximum injection time was increased to 50 ms; the scan range was set as *m/z* 100–800. For the targeted MS^2 scan, the Orbitrap detector was set up with a resolution of 240000; the normalized AGC target (%) was chosen as 1000 (5×10^5); the maximum injection time was 500 ms. Only the precursor ions of *m/z* 401.2 for N^6-HPB-dAdo and *m/z* 405.2 for [pyridine-D_4]N^6-HPB-dAdo were included for the MS^2 scan. Quantitation was performed using the MS^2 transition of $[M+H]^+ \rightarrow [M+H\text{-}dR]^+$.

For the calibration curve, the ratios of N^6-HPB-dAdo/[pyridine-D_4]N^6-HPB-dAdo were 0.5, 1, 2, 5, 10, with [pyridine-D_4]N^6-HPB-dAdo at a constant concentration of 0.1 fmol/μL in H_2O. The injection volume was 2 μL for each injection. The concentration range chosen was to cover the range of N^6-HPB-dAdo levels in rat liver and lung DNA samples. Low concentrations of N^6-HPB-dAdo were used for determining the limit of detection (LOD) to be 6.5 amol (on column). For the method validation of accuracy and precision, two amounts of N^6-HPB-dAdo (1 and 5 fmol) were spiked into 40 μg calf thymus DNA in succinate buffer with 1 fmol of [pyridine-D_4]N^6-HPB-dAdo added as the internal standard. These two amounts represent the low and high levels of N^6-HPB-dAdo in rat tissue samples. All the samples were prepared using the same method as described above. The recovery was 75%. The limit of quantitation (LOQ) was 200 amol (on column) as assessed by the lowest spiked level of N^6-HPB-dAdo in calf thymus DNA that produced a coefficient of variation (CV) of less than 10%. The determined levels of N^6-HPB-dAdo in the rat liver and lung DNA samples were calculated by the calibration curve, using the ratio of the peak areas of MS^2

quantitative transitions of N^6-HPB-dAdo and [pyridine-D_4]N^6-HPB-dAdo. All the MS data were processed using Thermo Xcalibur Qual Browser (version 4.3.73.11) software.

RESULTS

Three types of pyridyl dAdo-derived DNA adducts formed by NNN or NNK metabolism *in vivo* have been previously reported (Scheme 1 and Figure 1), but our understanding of adduct formation from these carcinogens is incomplete. In this study, we hypothesized that N^6-POB-dAdo (**11**), that has been observed in tissues of NNK-treated rats, and results from the intermediate **9** (Scheme 1), would be similarly formed by the same metabolite produced by NNN 2′-hydroxylation.

Preliminary study of dAdo-derived adduct formation *in vitro* and *in vivo*

Hydrolysates of liver and lung DNA of rats treated with 500 ppm racemic NNN in the drinking water for 3 weeks were first analyzed by MS using the LC method described in Table S2. As shown in Figure S6B, N^6-PHB-dAdo was barely observed in the $NaBH_3CN$-reduced sample from liver DNA of rats treated with 500 ppm racemic NNN. This was consistent with our previous observation when using a method with relatively low sensitivity.[15]

However, it was surprising to observe the formation of N^6-PHB-dAdo in calf thymus DNA incubated with 5′-acetoxyNNN, followed by $NaBH_3CN$ reduction, as confirmed by co-elution with its isotopically labelled internal standard [$^{15}N_5$]N^6-PHB-dAdo (Figure S6A). The presence of N^6-PHB-dAdo in calf thymus DNA incubated with 5′-acetoxyNNN, followed by reduction with $NaBH_3CN$, raised some questions regarding its precursor adduct, since N^6-POB-dAdo was not supposed to be formed by 5′-acetoxyNNN (Scheme 1) and was not observed in the same but unreduced sample (Figure S9C). Further study suggested that N^6-PHB-dAdo was formed by the reduction of N^6-[5-(3-pyridyl)tetrahydrofuran-2-yl]-2′-deoxyadenosine (N^6-Py-THF-dAdo) (Scheme S3), which had been previously observed only at the nucleoside level, e.g. in the reaction of 5′-acetoxyNNN with dAdo.[27] However, our present results described in the accompanying manuscript suggested that it is also present in calf thymus DNA incubated with 5′-acetoxyNNN but not in liver and lung DNA of rats treated with NNN.[29]

More surprisingly, a peak eluting only slightly earlier, at 22.3 min, than N^6-PHB-dAdo was observed both *in vitro* and *in vivo* after reduction with $NaBH_3CN$ (Figure S6). Fragmentation ions of *m/z* 136.0618 $[Ade+H]^+$ and *m/z* 150.0913 (pyridyl fragment) of MS^3 transitions of this new peak suggested one unknown type of pyridyl dAdo adduct (Figure S7). Based on the abundance of the first-generation and second-generation product ions, as well as our knowledge of NNN metabolism mechanisms, the chemical structure of this new peak was proposed to be N^6-HPB-dAdo (**14**, Scheme 1). It is structurally close to N^6-PHB-dAdo, consistent with their very close retention times and similar fragmentation patterns. To confirm the proposed structure, N^6-HPB-dAdo and its isotopically labelled internal standard [pyridine-D_4]N^6-HPB-dAdo were synthesized.

Synthesis and characterization of N^6-HPB-dAdo and [pyridine-D_4]N^6-HPB-dAdo

N^6-HPB-dAdo and [pyridine-D_4]N^6-HPB-dAdo were synthesized by a four-step procedure (Scheme 2). Conversion of the carbonyl group of **16** to the amino group of **18** was accomplished in two steps via the oxime intermediate. The final S_NAr reaction with **19** yielded the desired product N^6-HPB-dAdo (**14**). Its structure was confirmed by one- and two-dimensional NMR experiments (Figure S2) and HRMS. [Pyridine-D_4]N^6-HPB-dAdo was synthesized using the same method, and the structure was similarly confirmed (Figure S3).

Representative LC chromatograms of chemical standards N^6-HPB-dAdo and N^6-PHB-dAdo with their corresponding isotopically labelled internal standards are shown in Figure 2. Under the LC conditions described in Table S1, the peaks of N^6-HPB-dAdo elute slightly later than N^6-PHB-dAdo, with clear separation of the two diastereomers, in ratios near unity. It is noteworthy that the separation was easily compromised by changes of hand-packed column quality (Figure S8). Even though N^6-PHB-dAdo also has two diastereomers, no such separation was achieved under the conditions we have tried.

The pattern of the product ions of N^6-HPB-dAdo and [pyridine-D_4]N^6-HPB-dAdo agreed well with the proposed fragmentation pattern (Figure 2). The most abundant product ions in the MS^2 transitions were *m/z* 285.1459 [N^6-HPB-Ade+H]$^+$ and 289.1710 [[pyridine-D_4]N^6-HPB-Ade+H]$^+$. The product ion pattern of the MS^3 transition of each standard was also consistent with the proposed fragmentation pattern. The subtle difference of product ion patterns of both MS^2 and MS^3 transitions between N^6-HPB-dAdo and N^6-PHB-dAdo are also noted in Figure 2. The unique features of the MS^2 fragments *m/z* 267.1353 and 272.1204 of N^6-PHB-dAdo and [$^{15}N_5$]N^6-PHB-dAdo respectively were helpful to distinguish this adduct from N^6-HPB-dAdo in the rat DNA samples.

Investigation of N^6-PHB-dAdo *in vitro* and *in vivo* after reduction

Calf thymus DNA incubated with 5′-acetoxyNNN and treated with a reducing agent ($NaBH_4$ or $NaBH_3CN$) was analyzed by the new LC-NSI-HRMS/MS method. As shown in Figure 3B, N^6-PHB-dAdo was clearly formed *in vitro* upon $NaBH_4$ reduction. No such peak was observed in the $NaBH_4$-reduced untreated calf thymus DNA (Figure 3A). The same peak was also observed in the calf thymus DNA incubated with NNKOAc (Figure 3G) as previously reported.[18] The precursor compound of N^6-PHB-dAdo is considered to be N^6-Py-THF-dAdo (*vide supra*). No N^6-POB-dAdo was observed *in vitro* without reduction (Figure S9C), which agreed well with the metabolic mechanism of 5′-acetoxyNNN as depicted in Scheme S3.

In the liver and lung DNA of rats treated with racemic NNN, N^6-PHB-dAdo was formed upon $NaBH_4$ reduction (Figures 3D and 3F). No such peaks were observed in the control samples (Figures 3C and 3E). Consistent with our previous observations, N^6-PHB-dAdo was also formed in the lung DNA of rats chronically treated with 5 ppm NNK in the drinking water for 50 weeks (Figure 3H).[18] The precursor compound of N^6-PHB-dAdo *in vivo* is different from *in vitro*; it is N^6-POB-dAdo. As shown in Figures S9D and S9E, N^6-POB-dAdo co-eluted with its isotope labelled internal standard [pyridine-D_4]N^6-POB-dAdo

in the liver and lung DNA of rats treated with NNN. The formation of N^6-POB-dAdo in NNKOAc-treated calf thymus DNA and the liver DNA of rats treated with NNK was also reaffirmed as reported before (Figures S9A and S9B).[18]

It is noteworthy that N^6-PHB-dAdo was formed in very low levels upon $NaBH_3CN$ reduction of DNA from rats treated with NNN. The effect is clearly observed when comparing the levels of N^6-PHB-dAdo in the same rat liver and lung DNA samples, upon reduction of $NaBH_4$ (Figures 3D and 3F) versus $NaBH_3CN$ (Figures S10D and S10F). Since $NaBH_3CN$ was used for the previous study[15] which failed to observe the formation of N^6-PHB-dAdo, the insufficient conversion of N^6-POB-dAdo to N^6-PHB-dAdo by $NaBH_3CN$ reduction is likely to be one potential explanation.

Investigation of N^6-HPB-dAdo *in vitro* and *in vivo* after reduction

The formation of the new adduct N^6-HPB-dAdo was confirmed using its authentic synthesized internal standard [pyridine-D_4]N^6-HPB-dAdo. As shown in Figure 3B, this adduct was unambiguously formed *in vitro* upon $NaBH_4$ reduction of calf thymus DNA incubated with 5′-acetoxyNNN, co-eluting with [pyridine-D_4]N^6-HPB-dAdo. The MS^2 and MS^3 fragmentation patterns of the two peaks were also similar to the synthesized standard. The precursor compound of N^6-HPB-dAdo is considered to be N^6-[4-oxo-1-(pyridine-3-yl)butyl]-2′-deoxyadenosine (N^6-OPB-dAdo), in equilibration with 6-[2-(3-pyridyl)-*N*-pyrrolidinyl-5-hydroxy]-2′-deoxynebularine (Py-Py(OH)-dN), which has been observed *in vitro* and *in vivo* (Scheme S3).[29] No such peak was observed in the untreated (Figure 3A) or NNKOAc-treated calf thymus DNA (Figure 3G). This strongly indicates that N^6-HPB-dAdo is specifically formed by NNN metabolism. Both $NaBH_3CN$ and $NaBH_4$ were able to form N^6-HPB-dAdo by reduction. However, higher abundance of N^6-HPB-dAdo formed by the reduction of $NaBH_4$ than $NaBH_3CN$ was clearly observed (Figure 3 versus Figure S10). Thus, $NaBH_4$ reduction was chosen for the following quantitation study.

In the reduced DNA hydrolysates of rat liver and lung, N^6-HPB-dAdo was formed in relatively high abundance (Figures 3D and 3F). This adduct was not observed in the liver and lung DNA of rats from the control group (Figures 3C and 3E) or the lung DNA of rats treated with NNK (Figure 3H). The levels of N^6-HPB-dAdo in the liver and lung DNA of rats treated with NNN appeared to be 71- and 486-fold higher than N^6-PHB-dAdo, respectively, by estimating the MS responses and assuming similar ionization efficiencies of the two adducts (Figures 3D and 3F). Thus, it is of great interest to quantify the levels of N^6-HPB-dAdo in rat tissues such as liver and lung and compare to other DNA adducts specially formed by NNN metabolism.

Mass spectrometry quantitation of N^6-HPB-dAdo in liver and lung of rats treated with NNN

Our previous animal study provided the liver and lung tissues of rats treated with different doses of racemic NNN, which allowed us to investigate the dose-dependent response of N^6-HPB-dAdo to NNN exposure *in vivo*.[15] DNA hydrolysates were quantitatively analyzed for N^6-HPB-dAdo using the MS^2 transition of *m/z* 401.2 $[M+H]^+ \rightarrow$ 285.1458 $[M+H\text{-}dR]^+$. The quantitative MS method was validated with good accuracy and precision (Table 2).

The calibration curve for N^6-HPB-dAdo showed good linearity with an R^2 value of 0.9989 (Figure S11).

As depicted in Table 3, levels of N^6-HPB-dAdo in the liver DNA of rats ranged from 74 ± 4 to 233 ± 84 fmol/μmol dGuo (or from 49 ± 2 to 154 ± 55 fmol/mg DNA), and were roughly dose-dependent. The levels of N^6-HPB-dAdo in rat liver DNA were comparable to the levels of 2-[2-(3-pyridyl)-*N*-pyrrolidinyl]-2′-deoxyinosine (Py-Py-dI, Figure 1), the only NNN-specific DNA adduct quantified before,[15] in the same rat liver tissues. However, N^6-HPB-dAdo occurred in substantially lower abundance (~6 fold) in the rat lung DNA when compared with Py-Py-dI, ranging from 110 ± 18 to 328 ± 44 fmol/μmol dGuo (or from 73 ±12 to 217 ± 29 fmol/mg DNA).

DISCUSSION

This is the first study to characterize an NNN-specific dAdo adduct N^6-HPB-dAdo formed by this tobacco-specific carcinogen. Its structure was confirmed with authentic synthesized standards. This new adduct was observed both *in vitro* (calf thymus DNA treated with 5′-acetoxyNNN) and *in vivo* (liver and lung DNA from rats treated with NNN). Quantitation suggested a rough dose-dependent response of NNN treatment and the adduct level in rat liver and lung. N^6-HPB-dAdo is a new and structurally unique type of DNA adduct formed only by NNN 5′-hydroxylation.

The retention times of N^6-HPB-dAdo and the structurally similar adduct N^6-PHB-dAdo differed to a very small extent. Baseline separation was achieved under two different HPLC conditions. Using the preliminary HPLC method with 2 mM NH_4OAc and CH_3CN as the mobile phase (Table S2), N^6-HPB-dAdo eluted ~1.5 min earlier than N^6-PHB-dAdo (Figure S6). An optimized HPLC method using 0.05% formic acid in H_2O and CH_3CN as the mobile phase (Table S1) eluted N^6-HPB-dAdo ~0.1 min later than N^6-PHB-dAdo. This method also achieved a good separation of the two diastereomers of N^6-HPB-dAdo (Figure 2). The liquid chromatographic baseline separation of these two adducts, together with the unique MS^2 transition of *m/z* $[M+H]^+$ 401.1932 → $[M+H\text{-dR-}H_2O]^+$ 267.1353 of N^6-PHB-dAdo, provided unambiguous evidence for the formation of the new adduct N^6-HPB-dAdo in rat liver and lung. The difference of formation and persistence of the two diastereomers of N^6-HPB-dAdo was considered minor as shown in Figure 3. Thus, the absolute configuration of the two isomers and assignment of each peak were not pursued in this study.

In agreement with our hypothesis that the formation of N^6-POB-dAdo and N^6-PHB-dAdo (after reduction) should occur in the liver and lung DNA of rats by the treatment of NNN, those adducts were observed but in very low abundance. Levels of N^6-PHB-dAdo were estimated to be 71 and 486 folds lower than N^6-HPB-dAdo in the rat liver and rat lung, respectively (Figures 3D and 3F). This was likely the reason for not observing these adducts in our previous study[15] and highlighted the advantage of using the highly sensitive and specific LC-NSI-HRMS/MS method for investigating trace levels of DNA adducts in *in vivo* samples.

Levels of N^6-HPB-dAdo in the liver and lung DNA of rats treated with different doses of racemic NNN quantified by MS suggested a rough dose-dependent response to the NNN exposure. This result agreed with our previous study of Py-Py-dI.[15] Even though N^6-HPB-dAdo levels were comparable to Py-Py-dI in rat liver DNA, it occurred in substantially lower levels in rat lung DNA ranging from 110 ± 18 to 328 ± 44 fmol/μmol dGuo, when compared to Py-Py-dI which occurred in the levels of 580 ± 41 to 2018 ± 200 fmol/μmol dGuo. The low levels of N^6-HPB-dAdo may be due to the lower formation of this adduct by NNN. It is also possible that N^6-HPB-dAdo might be more prone to be repaired than Py-Py-dI, leading to relatively low levels of persistence in the lung. Considering that target tissues of NNN treatment in rats are mainly esophagus, oral mucosa and nasal mucosa,[11–13,23] quantitation of N^6-HPB-dAdo in those tissues will provide a better understanding of the persistence and distribution of this newly identified dAdo adduct. Levels of N^6-HPB-dAdo in comparison to those of Py-Py-dI in the target tissues of rats will be more important. A study is currently in progress to provide these tissues for analysis.

The formation of DNA adducts by the metabolic activation of the tobacco carcinogens NNN and NNK has been studied intensively.[30,31] However, only a few pyridyl dAdo-derived adducts have been observed *in vivo*. They were N^6-POB-dAdo and N^6-PHB-dAdo observed in rat lung and liver, and Py-Py-dN observed in rat lung and nasal cavity (structures shown in Scheme 1).[15,18] The new adduct N^6-HPB-dAdo reported in this study enlarges the repertoire of dAdo-derived adducts. More importantly, N^6-HPB-dAdo represents a new type of DNA adduct that is structurally specific to NNN treatment. As illustrated in Scheme 1, metabolic activation of NNN through 2′-hydroxylation forms the diazonium ion **9** which can also be formed by NNK bioactivation. Thus, the resulting dAdo adducts such as N^6-POB-dAdo and N^6-PHB-dAdo are not structurally specific to NNN or NNK metabolism. However, the new adduct N^6-HPB-dAdo characterized in this study is formed by the diazonium ion **10**, which is a specific metabolite of NNN 5′-hydroxylation. Considering previous findings that 5′-hydroxylation predominates in the metabolic activation of NNN in some cultured human tissues[32–36] and in the patas monkey,[37] the new adduct may be present in relatively higher abundance in human DNA samples. Similarly, we might expect dGuo and Thd to form analogous NNN-specific adducts such as N^2-HPB-dGuo/O^6-HPB-dGuo and O^2-HPB-Thd when treated with 5′-acetoxyNNN *in vitro* or NNN *in vivo*. These adducts could comprise a new group of DNA lesions that have not been biologically studied. They may also shed light on the current challenging studies directed toward identifying tobacco-specific DNA adducts in samples from human smokers and smokeless tobacco users.

The structural feature of N^6-HPB-dAdo also provides new insights for the investigation of activation biomarkers of NNN metabolism. The current biomarker used for evaluating NNN exposure in humans is urinary total NNN (free NNN plus its glucuronide derivative NNN-*N*-Gluc).[5,38] It was successfully applied to reveal a strong correlation between NNN exposure in human smokers' urine and future esophageal cancer incidence in the Shanghai Cohort study.[5] However, urinary total NNN does not necessarily reflect the metabolic fate of NNN. Previous study of NNN metabolism in the patas monkey suggested only less than 1% of intravenously dosed NNN was excreted unchanged in the urine.[37] This finding suggested that the majority of NNN injected into the patas monkey was biotransformed

to its metabolites. Most major NNN metabolites are identical to minor metabolites of nicotine, thus precluding their use as specific biomarkers of NNN exposure in people who use tobacco products.[39,40] Thus, it will potentially be beneficial to identify NNN-specific metabolites as activation biomarkers to evaluate NNN exposure and uptake for clinical trials. The formation of N^6-HPB-dAdo in rat liver and lung DNA indicates that adducted products can also be formed when the diazonium ion **10** from NNN 5′-hydroxylation reacts with various nucleophiles that are widely distributed in the body, e.g. glutathione, amino acids, or taurine. The adductive products, if formed and stable *in vivo*, may have the potential to serve as the surrogate biomarkers for monitoring exposure to, and bioactivation of NNN.

In summary, we have shown for the first time the formation of N^6-HPB-dAdo in the liver and lung DNA of rats treated with NNN using a highly sensitive and specific LC-NSI-HRMS/MS method. This represents a new type of DNA adduct specifically formed by NNN 5′-hydroxylation. The levels of this adduct in the liver and lung DNA of rats were roughly dose-dependent to the NNN treatment. The reported findings here lead to new insights for identifying tobacco-specific DNA adducts as well as investigating new activation biomarkers of NNN metabolism.

Supplementary Material

Refer to Web version on PubMed Central for supplementary material.

ACKNOWLEDGMENTS

The authors thank Drs. Erik S. Carlson, Adam T. Zarth and Pramod Upadhyaya for their input and preliminary work on this NNN project. We thank Drs. Peter W. Villalta and Yingchun Zhao for help with the operation of the mass spectrometer. We also thank Bob Carlson for his editorial assistance. Yupeng would like to thank Valeria Guidolin (Silvia Balbo lab) for her help with method validation and dGuo quantitation. Yupeng also appreciates Dr. Bin Ma for his valuable suggestions about mass spectrometric analysis.

Funding

This study was supported by grant CA-81301 from the National Cancer Institute. Mass spectrometry was carried out in the Analytical Biochemistry Shared Resource of the Masonic Cancer Center, University of Minnesota, supported in part by Cancer Center Support Grant CA-077598.

ABBREVIATIONS

NNN	N′-nitrosonornicotine
NNK	4-(methylnitrosamino)-1-(3-pyridyl)-1-butanone
dAdo	2′-deoxyadenosine
NNAL	4-(methylnitrosamino)-1-(3-pyridyl)-1-butanol
POB	pyridyloxobutryl
PHB	pyridylhydroxybutyl
Gua	guanine
Thd	thymidine

$NaBH_3CN$	sodium cyanoborohydride
LC-NSI-HRMS/MS	liquid chromatography-nano-electrospray ionization-high-resolution tandem mass spectrometry
HPLC	high performance liquid chromatography
SPE	solid phase extraction
i.d.	inner diameter
SIM	selected-ion monitoring
HCD	higher-energy collisional dissociation
AGC	automatic gain control
LOD	limit of detection
LOQ	limit of quantitation
CV	coefficient of variation
NL	normalizing level

REFERENCES

1. Islami F, Goding Sauer A, Miller KD, Siegel RL, Fedewa SA, Jacobs EJ, McCullough ML, Patel AV, Ma J, et al. (2018) Proportion and number of cancer cases and deaths attributable to potentially modifiable risk factors in the United States. CA Cancer J Clin 68, 31–54. [PubMed: 29160902]
2. International Agency for Research on Cancer. (2004) Tobacco smoke and involuntary smoking, In IARC Monographs on the Evaluation of Carcinogenic Risks to Humans, vol 83 pp 81–83.
3. Hecht SS (1998) Biochemistry, biology, and carcinogenicity of tobacco-specific *N*-nitrosamines. Chem Res Toxicol 11, 559–603. [PubMed: 9625726]
4. Hecht SS (2020) Metabolism and DNA adduct formation of carcinogenic tobacco-specific nitrosamines found in smokeless tobacco products, In Smokeless Tobacco Products: Characteristics, Usage, Health Effects, and Regulatory Implications (Pickworth WB, Ed.) pp 151–166, Elsevier, Amsterdam.
5. Yuan JM, Knezevich AD, Wang R, Gao YT, Hecht SS, and Stepanov I (2011) Urinary levels of the tobacco-specific carcinogen *N'*-nitrosonornicotine and its glucuronide are strongly associated with esophageal cancer risk in smokers. Carcinogenesis 32, 1366–1371. [PubMed: 21734256]
6. Stepanov I, Sebero E, Wang R, Gao YT, Hecht SS, and Yuan JM (2014) Tobacco-specific *N*-nitrosamine exposures and cancer risk in the Shanghai Cohort Study: remarkable coherence with rat tumor sites. Int J Cancer 134, 2278–2283. [PubMed: 24243522]
7. International Agency for Research on Cancer. (2007) Smokeless tobacco and some tobacco-specific *N*-nitrosamines, In IARC Monographs on the Evaluation of Carcinogenic Risks to Humans, v 89 pp 1–592, IARC, Lyon, FR. [PubMed: 18335640]
8. Wiencke JK (2002) DNA adduct burden and tobacco carcinogenesis. Oncogene 21, 7376–7391. [PubMed: 12379880]
9. Jalas JR, Hecht SS, and Murphy SE (2005) Cytochrome P450 enzymes as catalysts of metabolism of 4-(methylnitrosamino)-1-(3-pyridyl)-1-butanone, a tobacco specific carcinogen. Chem Res Toxicol 18, 95–110. [PubMed: 15720112]
10. Hecht SS, Lin D, Chuang J, and Castonguay A (1986) Reactions with deoxyguanosine of 4-(carbethoxynitrosamino)-1-(3-pyridyl)-1-butanone, a model-compound for α-hydroxylation of tobacco-specific nitrosamines. J Am Chem Soc 108, 1292–1295.

11. Lao Y, Yu N, Kassie F, Villalta PW, and Hecht SS (2007) Analysis of pyridyloxobutyl DNA adducts in F344 rats chronically treated with (*R*)- and (*S*)-*N'*-nitrosonornicotine. Chem Res Toxicol 20, 246–256. [PubMed: 17305408]
12. Zhang S, Wang M, Villalta PW, Lindgren BR, Lao Y, and Hecht SS (2009) Quantitation of pyridyloxobutyl DNA adducts in nasal and oral mucosa of rats treated chronically with enantiomers of *N'*-nitrosonornicotine. Chem Res Toxicol 22, 949–956. [PubMed: 19405515]
13. Zhao L, Balbo S, Wang M, Upadhyaya P, Khariwala SS, Villalta PW, and Hecht SS (2013) Quantitation of pyridyloxobutyl-DNA adducts in tissues of rats treated chronically with (*R*)- or (*S*)-*N'*-nitrosonornicotine (NNN) in a carcinogenicity study. Chem Res Toxicol 26, 1526–1535. [PubMed: 24001146]
14. Balbo S, Johnson CS, Kovi RC, James-Yi SA, O'Sullivan MG, Wang M, Le CT, Khariwala SS, Upadhyaya P, et al. (2014) Carcinogenicity and DNA adduct formation of 4-(methylnitrosamino)-1-(3-pyridyl)-1-butanone and enantiomers of its metabolite 4-(methylnitrosamino)-1-(3-pyridyl)-1-butanol in F-344 rats. Carcinogenesis 35, 2798–2806. [PubMed: 25269804]
15. Zarth AT, Upadhyaya P, Yang J, and Hecht SS (2016) DNA adduct formation from metabolic 5'-hydroxylation of the tobacco-specific carcinogen *N'*-nitrosonornicotine in human enzyme systems and in rats. Chem Res Toxicol 29, 380–389. [PubMed: 26808005]
16. Yang J, Villalta PW, Upadhyaya P, and Hecht SS (2016) Analysis of O^6-[4-(3-pyridyl)-4-oxobut-1-yl]-2'-deoxyguanosine and other DNA adducts in rats treated with enantiomeric or racemic *N'*-nitrosonornicotine. Chem Res Toxicol 29, 87–95. [PubMed: 26633576]
17. Leng J, and Wang Y (2017) Liquid chromatography-tandem mass spectrometry for the quantification of tobacco-specific nitrosamine-induced DNA adducts in mammalian cells. Anal Chem 89, 9124–9130. [PubMed: 28749651]
18. Carlson ES, Upadhyaya P, Villalta PW, Ma B, and Hecht SS (2018) Analysis and identification of 2'-deoxyadenosine-derived adducts in lung and liver DNA of F-344 rats treated with the tobacco-specific carcinogen 4-(methylnitrosamino)-1-(3-pyridyl)-1-butanone and enantiomers of its metabolite 4-(methylnitrosamino)-1-(3-pyridyl)-1-butanol. Chem Res Toxicol 31, 358–370. [PubMed: 29651838]
19. Guo S, Leng J, Tan Y, Price NE, and Wang Y (2019) Quantification of DNA lesions induced by 4-(methylnitrosamino)-1-(3-pyridyl)-1-butanol in mammalian cells. Chem Res Toxicol 32, 708–717. [PubMed: 30714728]
20. Ma B, Villalta PW, Zarth AT, Kotandeniya D, Upadhyaya P, Stepanov I, and Hecht SS (2015) Comprehensive high-resolution mass spectrometric analysis of DNA phosphate adducts formed by the tobacco-specific lung carcinogen 4-(methylnitrosamino)-1-(3-pyridyl)-1-butanone. Chem Res Toxicol 28, 2151–2159. [PubMed: 26398225]
21. Ma B, Zarth AT, Carlson ES, Villalta PW, Stepanov I, and Hecht SS (2017) Pyridylhydroxybutyl and pyridyloxobutyl DNA phosphate adduct formation in rats treated chronically with enantiomers of the tobacco-specific nitrosamine metabolite 4-(methylnitrosamino)-1-(3-pyridyl)-1-butanol. Mutagenesis 32, 561–570. [PubMed: 29186507]
22. Ma B, Zarth AT, Carlson ES, Villalta PW, Upadhyaya P, Stepanov I, and Hecht SS (2018) Identification of more than 100 structurally unique DNA-phosphate adducts formed during rat lung carcinogenesis by the tobacco-specific nitrosamine 4-(methylnitrosamino)-1-(3-pyridyl)-1-butanone. Carcinogenesis 39, 232–241. [PubMed: 29194532]
23. Li Y, Ma B, Cao Q, Balbo S, Zhao L, Upadhyaya P, and Hecht SS (2019) Mass spectrometric quantitation of pyridyloxobutyl DNA phosphate adducts in rats chronically treated with *N'*-nitrosonornicotine. Chem Res Toxicol 32, 773–783. [PubMed: 30740971]
24. Yun BH, Rosenquist TA, Nikolić J, Dragičević D, Tomić K, Jelaković B, Dickman KG, Grollman AP, and Turesky RJ (2013) Human formalin-fixed paraffin-embedded tissues: an untapped specimen for biomonitoring of carcinogen DNA adducts by mass spectrometry. Anal Chem 85, 4251–4258. [PubMed: 23550627]
25. Wilson MR, Jiang Y, Villalta PW, Stornetta A, Boudreau PD, Carrá A, Brennan CA, Chun E, Ngo L, et al. (2019) The human gut bacterial genotoxin colibactin alkylates DNA. Science 363, eaar7785. DOI: 10.1126/science.aar7785, [PubMed: 30765538]

26. Marriner GA, and Kerwin SM (2009) An improved synthesis of (+/−)-*N'*-nitrosonornicotine 5'-acetate. J Org Chem 74, 2891–2892. [PubMed: 19271724]
27. Upadhyaya P, and Hecht SS (2008) Identification of adducts formed in the reactions of 5'-acetoxy-*N'*-nitrosonornicotine with deoxyadenosine, thymidine, and DNA. Chem Res Toxicol 21, 2164–2171. [PubMed: 18821782]
28. Miao L, DiMaggio SC, and Trudell ML (2010) Hydroxyarylketones via ring-opening of lactones with aryllithium reagents: An expedient synthesis of (±)-anabasamine. Synthesis 2010, 91–97.
29. Li Y, Carlson ES, Zarth AT, Upadhyaya P, and Hecht SS Investigation of 2′-deoxyadenosine-derived adducts specifically formed in rat liver and lung DNA by *N'*-nitrosonornicotine (NNN) metabolism. Chem Res Toxicol submitted.
30. Yu Y, Wang P, Cui Y, and Wang Y (2018) Chemical analysis of DNA damage. Anal Chem 90, 556–576. [PubMed: 29084424]
31. Ma B, Stepanov I, and Hecht SS (2019) Recent studies on DNA adducts resulting from human exposure to tobacco smoke. Toxics 7, 16, doi: 10.3390/toxics7010016.
32. Hecht SS, Chen CH, McCoy GD, Hoffmann D, and Domellöf L (1979) Alpha-hydroxylation of *N*-nitrosopyrrolidine and *N'*-nitrosonornicotine by human liver microsomes. Cancer Lett 8, 35–41. [PubMed: 509417]
33. Castonguay A, Stoner GD, Schut HA, and Hecht SS (1983) Metabolism of tobacco-specific *N*-nitrosamines by cultured human tissues. Proc Natl Acad Sci 80, 6694–6697. [PubMed: 6579555]
34. Chakradeo PP, Nair J, and Bhide SV (1995) Metabolism of *N'*-nitrosonornicotine by adult and fetal human oesophagal cultures. Cell Biol Int 19, 53–58. [PubMed: 7613511]
35. Patten CJ, Smith TJ, Friesen MJ, Tynes RE, Yang CS, and Murphy SE (1997) Evidence for cytochrome P450 2A6 and 3A4 as major catalysts for *N'*-nitrosonornicotine alpha-hydroxylation by human liver microsomes. Carcinogenesis 18, 1623–1630. [PubMed: 9276639]
36. Jalas JR, Ding X, and Murphy SE (2003) Comparative metabolism of the tobacco-specific nitrosamines 4-(methylnitrosamino)-1-(3-pyridyl)-1-butanone and 4-(methylnitrosamino)-1-(3-pyridyl)-1-butanol by rat cytochrome P450 2A3 and human cytochrome P450 2a13. Drug Metab Dispos 31, 1199–1202. [PubMed: 12975327]
37. Upadhyaya P, Zimmerman CL, and Hecht SS (2002) Metabolism and pharmacokinetics of *N'*-nitrosonornicotine in the patas monkey. Drug Metab Dispos 30, 1115–1122. [PubMed: 12228188]
38. Stepanov I, and Hecht SS (2005) Tobacco-specific nitrosamines and their pyridine-*N*-glucuronides in the urine of smokers and smokeless tobacco users. Cancer Epidemiol Biomarkers Prev 14, 885–891. [PubMed: 15824160]
39. Hecht SS, Hatsukami DK, Bonilla LE, and Hochalter JB (1999) Quantitation of 4-oxo-4-(3-pyridyl)butanoic acid and enantiomers of 4-hydroxy-4-(3-pyridyl)butanoic acid in human urine: a substantial pathway of nicotine metabolism. Chem Res Toxicol 12, 172–179. [PubMed: 10027795]
40. Trushin N, and Hecht SS (1999) Stereoselective metabolism of nicotine and tobacco-specific *N*-nitrosamines to 4-hydroxy-4-(3-pyridyl)butanoic acid in rats. Chem Res Toxicol 12, 164–171. [PubMed: 10027794]

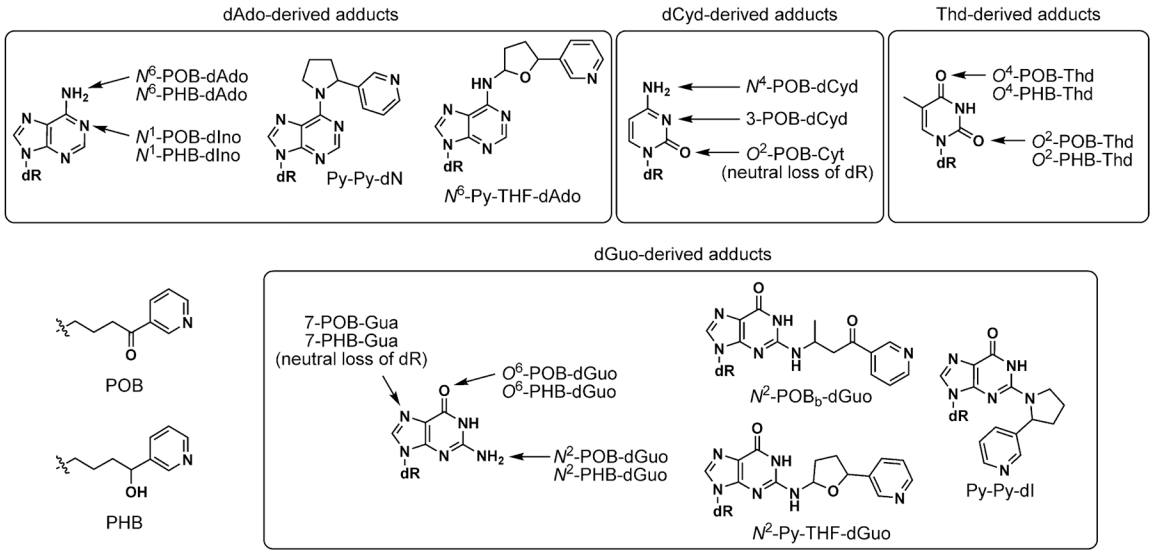

Figure 1.

Summary of previously investigated pyridyl DNA base adducts formed by NNN and NNK metabolism *in vitro* and *in vivo*. dR = 2′-deoxyribose.

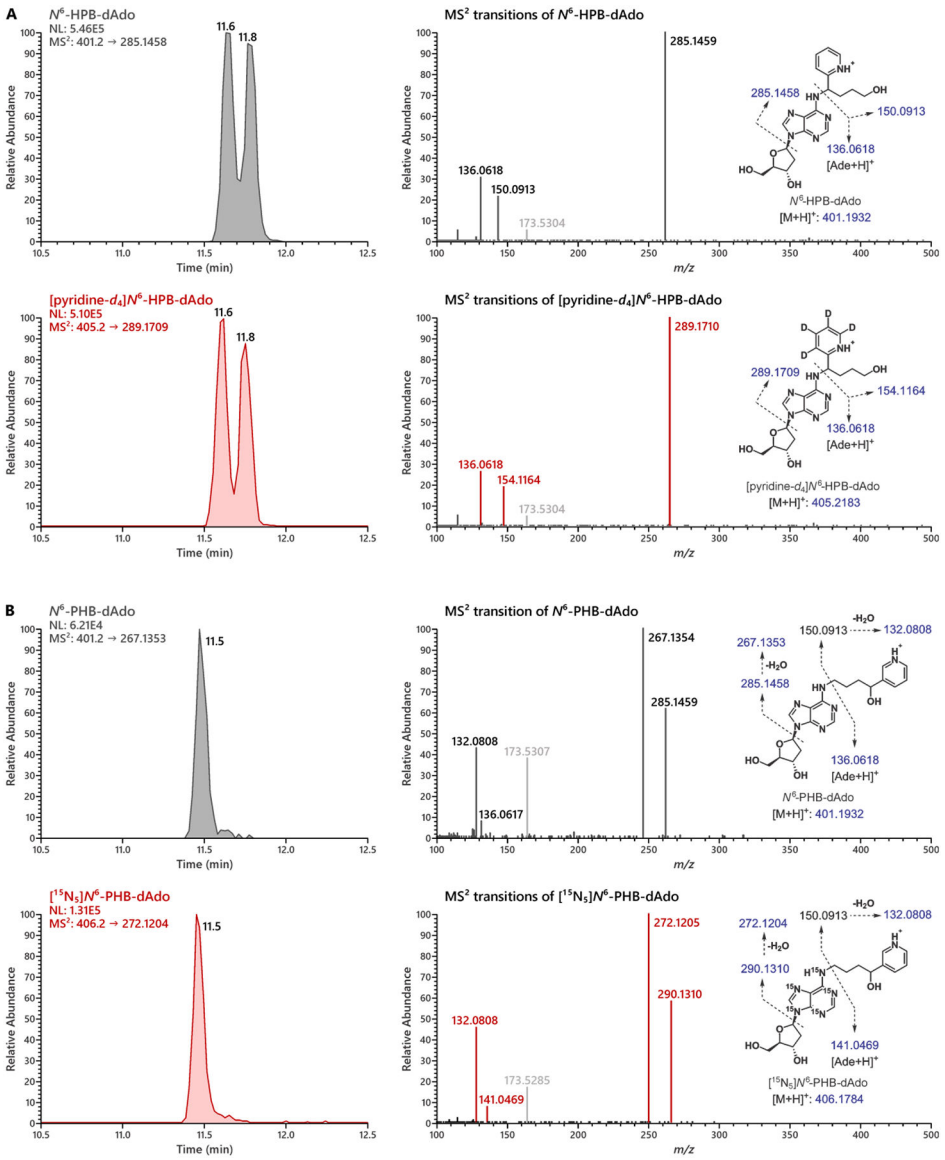

Figure 2.

Representative chromatograms and MS^2 product ion spectra of N^6-HPB-dAdo and [pyridine-D_4]N^6-HPB-dAdo versus N^6-PHB-dAdo and [$^{15}N_5$]N^6-PHB-dAdo. All the results agreed well with the proposed fragmentation patterns of the four chemical standards. The ion *m/z* 173.53 was a co-eluting interfering ion.

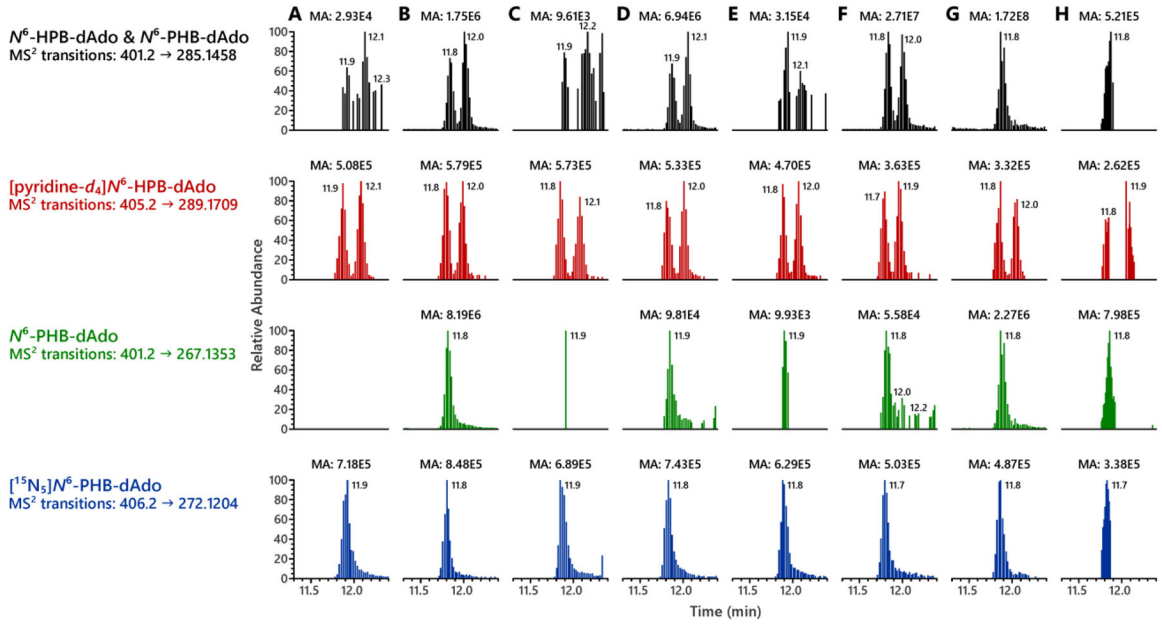

Figure 3.

Representative extracted product ion chromatograms of MS^2 transitions for the analysis of N^6-HPB-dAdo and N^6-PHB-dAdo formation in DNA samples upon $NaBH_4$ reduction. (A) Blank calf thymus DNA, (B) calf thymus DNA incubated with 5′-acetoxyNNN, (C) liver DNA of rat from the control group, (D) liver DNA of rats treated with 500 ppm racemic NNN for 3 weeks, (E) lung DNA of rat from the control group, (F) lung DNA of rats treated with 500 ppm racemic NNN for 3 weeks, (G) calf thymus DNA incubated with NNKOAc, and (H) lung DNA of rats treated with 5 ppm NNK for 70 weeks.

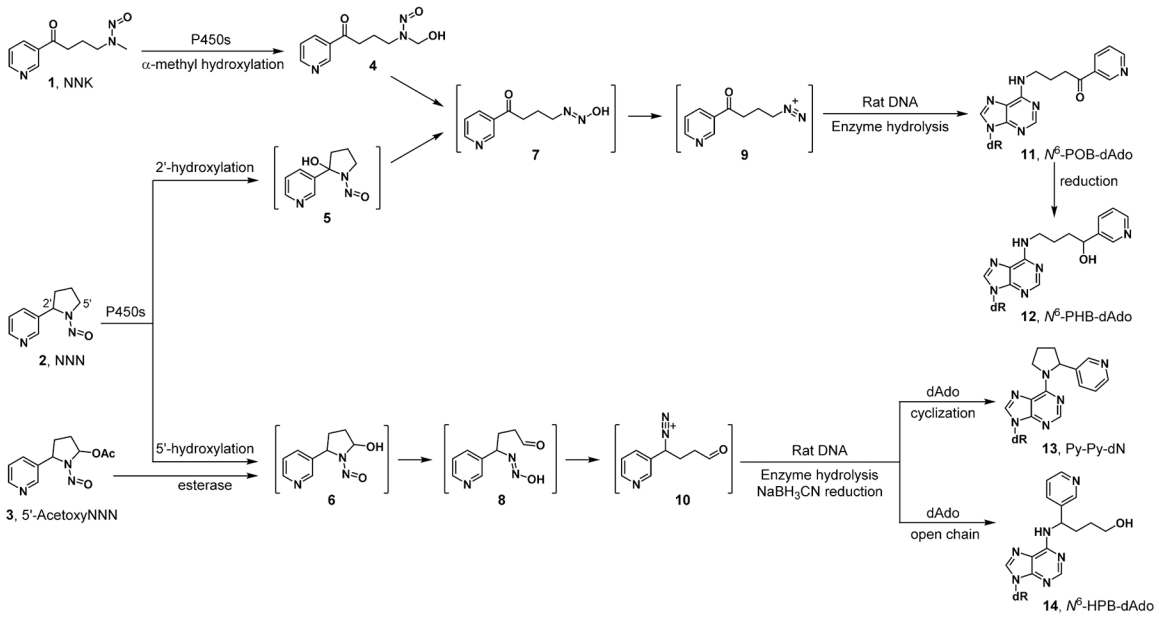

Scheme 1.

Mechanisms of NNN and NNK metabolic activation leading to dAdo-derived adducts in DNA.

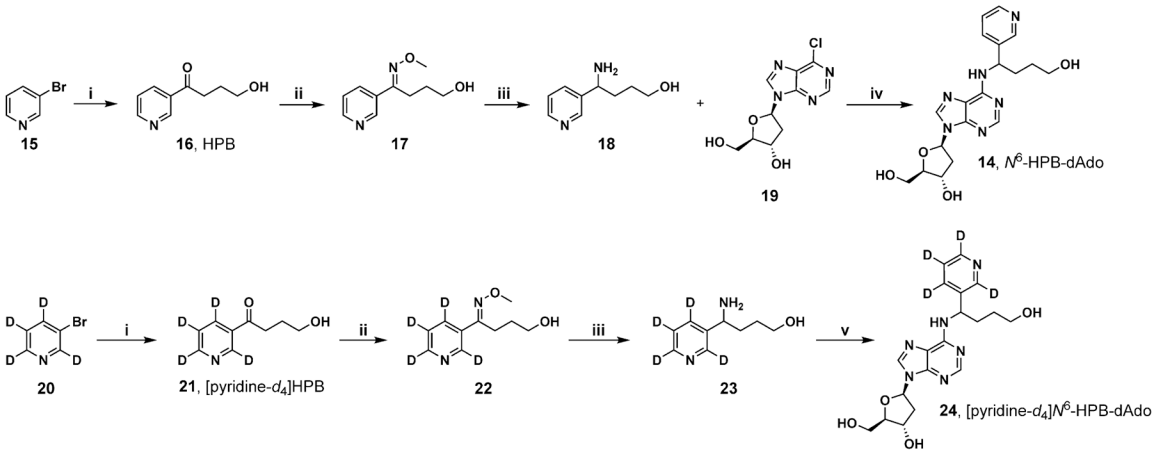

Scheme 2.
Synthetic routes for N^6-HPB-dAdo and [pyridine-D_4]N^6-HPB-dAdo.

Table 1.

Exact masses of target analytes and their most abundant first-generation and second-generation product ions.

Analyte	Parent ion $[M + H]^+$ (*m/z*)	First-generation product ions $[MS^2$ transition + $H]^+$ (*m/z*)	Second-generation product ions $[MS^3$ transition + $H]^+$ (*m/z*)
N^6-HPB-dAdo	401.1932	285.1458	150.0913; 136.0618
[pyridine-D_4]N^6-HPB-dAdo	405.2183	289.1709	154.1164; 136.0618
N^6-PHB-dAdo	401.1932	285.1458; 267.1353	136.0618; 132.0808
[$^{15}N_5$]N^6-PHB-dAdo	406.1784	290.1310; 272.1204	141.0469; 132.0808
N^6-POB-dAdo	399.1775	283.1302; 265.1196	148.0757; 136.0618
[pyridine-D_4]N^6-POB-dAdo	403.2026	287.1553; 269.1447	152.1008; 136.0618

Table 2.

Inter-day precision and accuracy for the mass spectrometry quantitation of N^6-HPB-dAdo.

Spiked (fmol)	Experiment	Measured (fmol)	Accuracy	Precision (CV)
1	Day 1	0.99		
	Day 2	1.14		
	Day 3	1.11		
	Mean ± SD	1.08 ± 0.08	108%	7.2%
5	Day 1	6.36		
	Day 2	5.63		
	Day 3	5.75		
	Mean ± SD	5.92 ± 0.39	118%	6.6%

Table 3.

Levels of N^6-HPB-dAdo and Py-Py-dI (fmol/μmol dGuo) in the DNA of liver and lung of rats (N = 3 per dose) treated with different doses of racemic NNN in the drinking water for 3 weeks.

DNA adduct	Rat tissue	Dose of racemic NNN		
		50 ppm	100 ppm	500 ppm
N^6-HPB-dAdo	liver	74 ± 4	84 ± 20	233 ± 84
	lung	110 ± 18	176 ± 34	328 ± 44
Py-Py-dI[a]	liver	56 ± 14	157 ± 42	412 ± 53
	lung	580 ± 41	1045 ± 69	2018 ± 200

[a]Data for Py-Py-dI levels in the same rat tissues were adapted from our previous study.[15]